MR Imaging in the Tethered Spinal Cord Syndrome

Narasimhachari Raghavan, A. James Barkovich, Michael Edwards and David Norman

AJNR Am J Neuroradiol 1989, 10 (1) 27-36
http://www.ajnr.org/content/10/1/27

MR Imaging in the Tethered Spinal Cord Syndrome

Narasimhachari Raghavan[1]
A. James Barkovich[1]
Michael Edwards[2]
David Norman[1]

MR examinations of the spine were reviewed in 25 patients with a clinical diagnosis of tethered spinal cord. In 21 patients (84%), the level of the tip of the conus was below the mid L2 vertebral body. The causes of the tethering were spinal lipomas (72%), tight filum terminale syndrome (12%), diastematomyelia (8%), and myelomeningocele (8%). These entities were readily identified in all instances. Bony dysraphisms were well demonstrated by MR. Interestingly, cavitary lesions/myelomalacia of the conus or the cord adjacent to the tethering lesion were seen with appropriate images in nine of 20 patients. This unexpected finding may have diagnostic and/or prognostic significance.

Spinal MR was found to be extremely useful in the evaluation of the suspected tethered spinal cord. It was able to visualize the conus medullaris, assess the thickness of the filum terminale, identify traction lesions, and evaluate associated bony dysraphisms.

Tethered spinal cord syndrome is often suspected clinically when patients present with motor and sensory dysfunction of lower extremities (unrelated to myotomal or dermatomal pattern), muscle atrophy, decreased or hyperactive reflexes, urinary incontinence, spastic gait, or orthopedic deformities such as scoliosis or foot deformities [1, 2]. Radiographic studies are used to confirm the presence of tethered cord, to ascertain the cause of tethering, and to rule out other diagnostic considerations such as neoplasms, disk herniations, and syringohydromyelia. Traditionally, positive-contrast myelography has been the diagnostic procedure of choice, often supplemented by CT with intrathecal contrast material. With the increasing sophistication of surface-coil technology, MR imaging has been shown to be of considerable value in the diagnosis of intrinsic spinal cord disease [2, 3]. In this article, we report our experience with the MR appearance of suspected tethered spinal cord syndrome.

Materials and Methods

MR examinations of 25 patients with the clinical diagnosis of tethered spinal cord were reviewed retrospectively. The 14 males and 11 females were 0–65 years old (mean, 18 years). All MR scans were obtained before surgical repair. Clinical findings included a fatty lump in the lower lumbosacral region without neurologic deficits, neurogenic bladder with urinary retention, urinary incontinence, decreased perianal sensation, numbness in lower extremities, spastic gait, and lower extremity pain (Table 1). The location of the conus medullaris was identified on axial and sagittal scans. Whenever possible the diameter of the filum terminale at the L5–S1 level was measured. In six cases, tethering was not associated with a well-defined filum. In three cases, images at the L5–S1 level were not available.

The cord was evaluated for the presence or absence of syringohydromyelia/myelomalacia. The cause of tethering was identified. Dysraphic abnormalities of the vertebral bodies and abnormalities of the spinal curvature were characterized. The relative difficulty involved in characterizing the osseous abnormalities was subjectively recorded. The position of the cerebellar tonsils was noted whenever scans at the foramen magnum level were available.

This article appears in the January/February 1989 issue of *AJNR* and the April 1989 issue of *AJR*.

Received March 21, 1988; accepted after revision June 17, 1988.

[1] Department of Radiology, Section of Neuroradiology, L–371, University of California, 505 Parnassus Ave., San Francisco, CA 94143. Address reprint requests to N. Raghavan.

[2] Department of Neurosurgery, University of California, San Francisco, CA 94143.

***AJNR* 10:27–36, January/February 1989**
0195–6108/89/1001–0027

TABLE 1: Summary of Patients with Tethered Spinal Cord Syndrome

Dysplasia: Case No.	Age	Gender	Conus Level		Filum Thickness (mm)	Syrinx/ Myelomalacia	Skeletal Abnormalities	Clinical Presentation
			Sagittal View	Axial View				
Spinal lipoma[a]:								
1	3	M	Mid L1	Mid L1	No axial view	Poor image	Normal T12–L4	R/O tethered cord
2	37	F	L2–L3	L2–L3	5	No	Normal	Dysesthesias both legs
3	0.6	M	S1	No axial view	No axial view	No axial view	No axial view	Fatty mass over lumbosacral spine
4	51	F	Not available	Not available	7	No	Normal L4–S1	Pain in both legs
5	37	M	Mid L3	Mid L3	Cord ends in lesion	No	Normal	Voiding difficulty
6	3	F	Mid–lower L2	Mid L2	3	No	Scoliosis Abnormal; poorly evaluable	Urinary incontinence Decreased perianal sensation
7	60	M	Mid L3	Mid L3	3	No	Sacral spina bifida	Neurogenic bladder
8	17	F	L3	No axial view	No axial view	No	No axial view	Numbness in L leg; atrophy
9	0.1	M	L3–L4	L3–L4	Cord ends in lesion	Yes	Spina bifida, L5 & S1	Neurogenic bladder; fatty mass over spine
10	0.3	M	L2–L3	L3–L4	4	Yes	Spina bifida, L5 & S1	Fatty mass over lumbosacral spine
11	65	M	L3–L4	No axial view	5	No axial view	Minimal scoliosis No axial view	R/O tethered cord
12	52	M	Mid L1	Mid L1	5	No	Normal	Dysesthesias, both legs
13	37	F	L5–S1	L5–S1	4	Yes	Spina bifida, L5 through sacrum	Numbness in feet; neurogenic bladder
14	1.3	F	L5	L5	3	Poor image	Spina bifida, L5 & S1	R/O tethered cord
15	3	M	L5–S1	L5–S1	Cord ends in lesion	Yes	Spina bifida, L5 & S1	Neurogenic bladder
16	12	F	L5–S1	L4–L5	2	No axial view	Mildly asymmetric spina bifida, L4; widely bifid L5 & S1	Urinary incontinence; dysesthesias in both legs
17	8	M	L5–S1	L5–S1	6	No	Scoliosis; dysraphic at L3–S1	R/O tethered cord
18	11	F	S1	S1	Cord ends in lesion	Yes	Sacral spina bifida	Toe walking; spasticity
None:								
19	16	M	L4–L5	L4–L5	5	Yes	Congenital fusion, L5 & S1; spina bifida occulta, L5; partial sacral agenesis	R/O tethered cord
20	7	F	Lower L3	Lower L3	4	Yes	Normal	R/O tethered cord
21	5	M	L1–L2	L1–L2	3	Yes	Spina bifida, L5–sacrum	Urinary incontinence
Myelomeningocele:								
22	4	F	Cord ends in myelomeningocele	Cord ends in myelomeningocele	–	No	No axial view	R/O tethered cord
23[b]	0	F	L5–S1	L5–S1	Not seen	No	Poorly evaluable	Decreased perianal sensation
Diastematomyelia:								
24	5	M	L4–L5	Not evaluable	3	No	Scoliosis; hemivertebrae; thick lamina with eversion; bony septum at L2	Hyperreflexia; hemispastic gait; positive Babinski test
25	Age not available	M	Mid L4	L4–L5	5	Yes	No bony septum; spina bifida of L5 & S1	R/O tethered cord

Note.—R/O = rule out; L = left.

[a] Comprises subtypes lipomyelomeningocele, intramedullary lipoma, and lipoma of filum terminale.

[b] Skin-covered.

All measurements and observations were made from the hard-copy images by using calipers and the relative MR scale generated on each image.

Most patients were examined on a 1.5-T whole body superconductive magnet* by using surface receiving coils; two patients were studied on a 0.35-T magnet.† Spin-echo sequences were used and data were acquired with either 128 or 256 views in the phase-encoding direction, 256 views in the read-out direction, and two to four excitations by using the two-dimensional Fourier transform method. The field of view was variable but ranged from 20 to 30 cm depending on the plane of imaging. Sagittal T1-weighted images, 600–1000/20–50 (TR/TE), with 3- to 5-mm section thickness were obtained in all patients. Five-millimeter axial spin-echo sections, 1000/20, were also available for 23 of 25 patients. The patients were supine during the examination.

Results

Level of Conus

The level of the conus could be determined in 23 of the 25 patients. In 19 cases, the level of the conus could be identified on both axial and sagittal views. Determination of the level of the conus on axial compared with sagittal views did not vary by more than one-half the vertebral body height in 17 patients and was discrepant by one vertebral body height in two (Table 1; Fig. 1). In five cases, no axial images through the conus tip were available; in one case, the conus was not visualized with certainty on either view owing to the presence of a traction lesion.

In 21 patients, the level of the conus was below the mid L2 vertebral body. In four (16%) of 25 patients, the tip of the conus was at or above the mid L2 level on axial images (Tables 1 and 2; Fig. 2). Three of these four patients had a spinal lipoma and the other had a thickened filum (normal is 2 mm or less). Cerebellar tonsillar ectopia was present in five of nine patients imaged at this level.

Cause of Tethering

The causes of the tethering are listed in Table 3. Intramedullary lipomas, lipomyelomeningoceles, and lipomas of the filum terminale are collectively referred to as spinal lipomas [4]. The distribution of the lesions in our study differs from the series of 71 patients reported by James and Lassman [5], in which spinal lipomas alone accounted for tethering in only 27% of patients while diastematomyelia was present in 34%.

The tethering lesions were identified readily on the MR studies, as the high signal intensity of fat is easily separable

TABLE 2: Level of Tip of Conus in Patients with Tethered Spinal Cord Syndrome

Level	No. of Patients	
	Sagittal Image	Axial Image
L1	2	2
L1–L2	1	1
L2	1	1
L2–L3	2	1
L3	4	3
L3–L4	2	2
L4	1	0
L4–L5	2	3
L5	1	1
L5–S1	5	4
S1	2	1

* General Electric, Milwaukee, or Philips Medical Systems, Shelton, CT.
† Diasonics, Milpitas, CA.

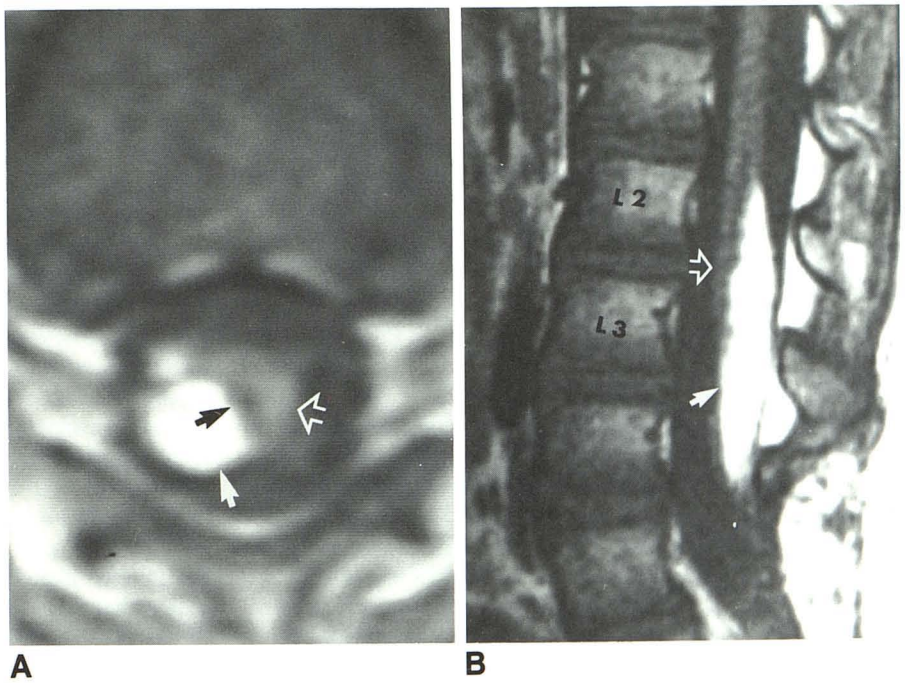

Fig. 1.—Case 10: 3-month-old boy with fatty mass over lower lumbosacral spine.

***A*, Axial spin-echo image, 1000/20, shows cord (*open arrow*) terminating in lipoma (*solid white arrow*) opposite L3–L4 disk-space level. Syringohydromyelic cavity/myelomalacia is present in terminal cord (*black arrow*).**

***B*, Midsagittal spin-echo image, 1000/20. As spinal cord (*open arrow*) is displaced laterally by lipoma (*solid arrow*), tip of conus falsely appears to be at L2–L3 level.**

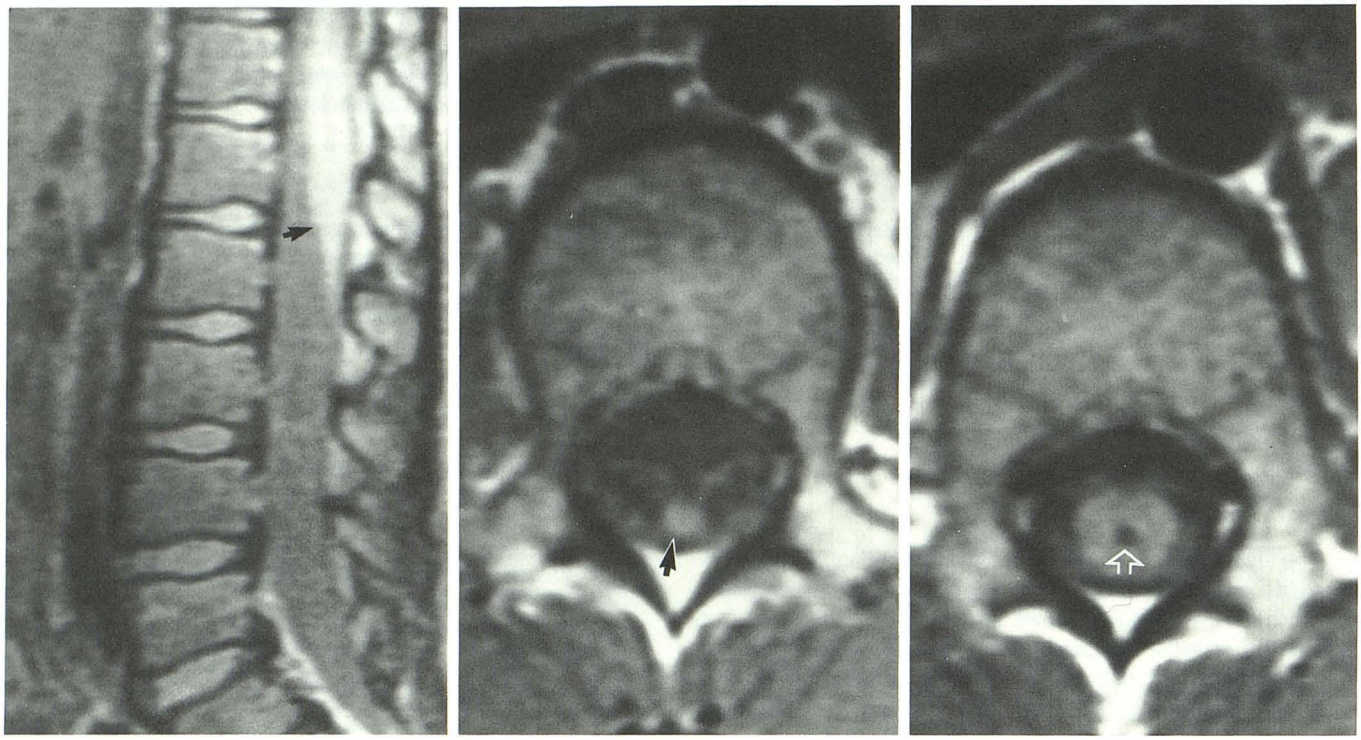

Fig. 2.—Case 21: 5-year-old boy with urinary incontinence.
***A* and *B*, Spin-echo sagittal, 1000/40 (*A*) and axial, 1000/20 (*B*), images confirm position of tip of conus (*arrows*) to be at L1–L2 interspace.**
***C*, Only other radiographic clue is syringohydromyelic cavity/myelomalacia (*arrow*) (possibly seen on sagittal image as well) from mid T11 to L1–L2 region.**

TABLE 3: Causes of Tethering in Tethered Spinal Cord Syndrome

Cause	No. of Patients (%)
Spinal lipoma	18 (72)
Thickened filum (>2 mm) without fat signal	3 (12)
Diastematomyelia	2 (8)
Myelomeningocele	2 (8)
Total	25 (100)

from the signal of the cord and of CSF on short TR/TE images (Fig. 3).

Filum Terminale

Normal filum thickness is stated to be 2 mm or less [6, 7]. Measurements were performed on axial images at the level of the L5–S1 interspace (Fig. 4), and, when clearly separable, the lipomatous elements were excluded from the determination of the filum thickness. In nine of 25 patients, filum thickness could not be measured. In five of these patients, either the cord ended in the traction lesion or the lesion prevented clear visualization of filum terminale. In one case, the filum could not be differentiated from nerve roots of cauda equina; in the remaining three, the scans did not include the L5–S1 interspace. The filum was greater than 2 mm in diameter in 15 of the 16 patients in whom it could be identified. In the sixteenth patient, the filum measured only 2 mm in width, and in this patient the conus was low-lying, positioned at the L4 vertebral body level.

Cord Architecture

The internal architecture of the spinal cord, judged subjectively on the ability to differentiate gray from white matter, was not well imaged in 20 patients. Nine of 25 subjects had a focal short-length low-intensity lesion representing either a syringohydromyelic cavity or a focus of myelomalacia, measuring 1–4 cm in length and 1–5 mm in diameter in the conus or in the cord adjacent to the tethering lesion if one was present (Fig. 1). These lesions could not be seen with any degree of confidence in the sagittal plane (Fig. 5). Adequate axial images through the cord were not available in five patients; of the 20 subjects with adequate images, nine demonstrated a focal low-intensity cord abnormality. On the short TR/TE axial images, they could be noted with confidence; their signal was similar to that of CSF and lower than that of spinal gray matter. The presence of gliosis or CSF "flow" void could not be evaluated because T2-weighted

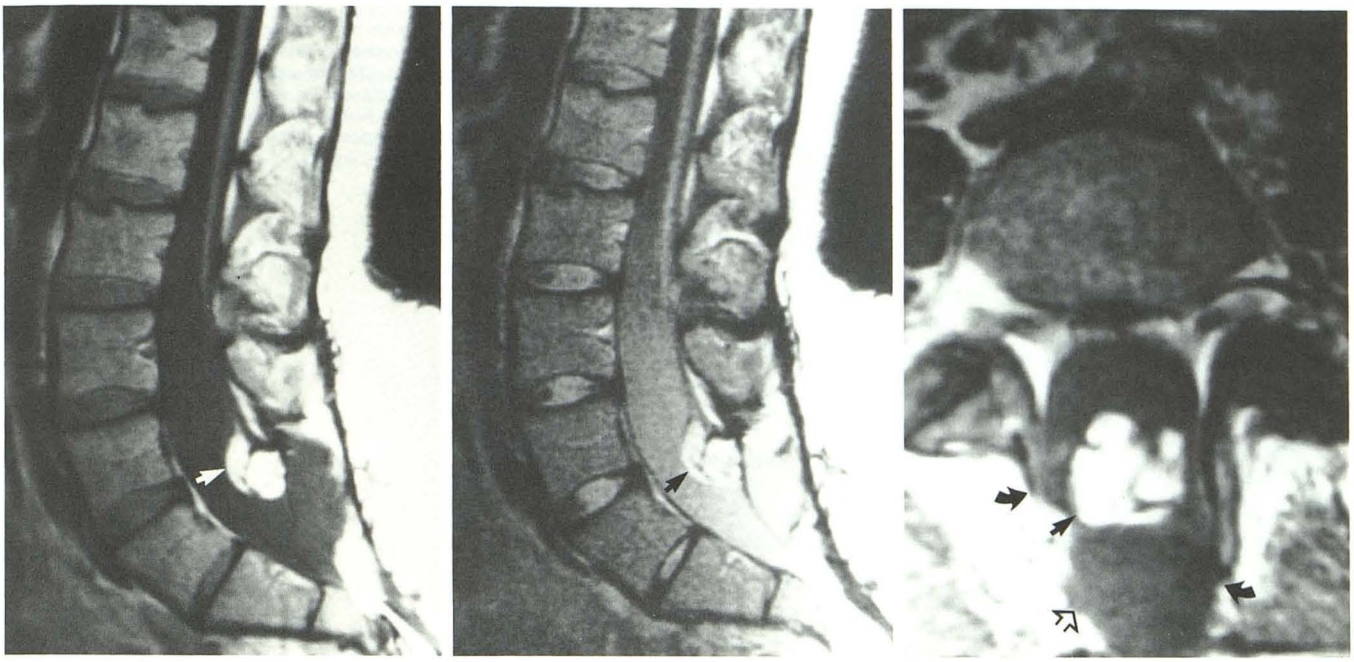

Fig. 3.—Case 2: 37-year-old woman with tethered spinal cord syndrome.
***A*, Sagittal spin-echo image, 1000/20, depicts low-lying conus tethered by high-intensity lipoma (*arrow*).**
***B*, Signal of lipoma (*arrow*) decreases on second echo of sequence, 1000/70.**
***C*, Axial spin-echo image, 1000/20. Bony detail is clearly visualized. Spina bifida (*curved arrows*), meningocele (*open arrow*), and lipoma (*solid straight arrow*) are evident.**

studies were not performed. Sagittal MR was performed at the craniocervical junction in four of the nine patients; none had evidence of a Chiari malformation. Scoliosis was not evident in any of these nine patients.

Bony Detail

In 19 of 25 patients, the vertebral architecture was easily characterized. In four patients, axial images were not available for evaluation; in two patients, the presence of a bony abnormality could be appreciated but was not well defined. Six studies demonstrated no bony abnormalities in the region imaged. Both patients with diastematomyelia had thickened, dysplastic, everted laminae. One of the two had a hemivertebra resulting in scoliosis, and a demonstrable bony diastematomyelic septum, shown to be osseous on plain films (Fig. 6). Congenital fusion of L5 and S1, partial sacral agenesis, spina bifida occulta at L5, and frank spina bifida at S1 and S2 were noted in one patient. The remaining 10 patients had spina bifida with varying degrees of laminar eversion. Scoliosis was noted in four subjects; syringohydromyelia/myelomalacia in the terminal cord could not be demonstrated in any of these patients.

Discussion

The spinal cord develops in a relatively orderly manner by the processes of neurulation and disjunction (Fig. 7). Inferior to the caudal neuropore, the neural tube elongates by canalization and retrogressive differentiation, ultimately forming the distalmost conus medullaris, the ventriculus terminalis, and the filum terminale [7, 8]. Full discussion of the embryology of spinal cord and column formation is beyond the scope of this article, and the interested reader is referred to several excellent discussions on the subject [7, 10–13].

The spinal cord "ascends" relative to the vertebral column because of the differential growth rates of the spinal cord and the vertebral column [6]. The rate of ascent of the conus medullaris is most rapid before the 17th week of gestation, during which period the cord ascends to terminate at the L4 level. Thereafter, the ascent proceeds at a slower pace, reaching the adult level in most patients approximately 2 months after birth [1]. Even though slower ascent can be seen normally, a conus level lower than mid L2 at an age greater than 12 years generally is accepted as abnormal [6]. To achieve the "ascent," the spinal cord must be free from the bony canal and the surrounding subcutaneous tissue [11]. The filum terminale, as previously mentioned, elongates as a result of retrogressive differentiation and is accompanied by an increase in the length of nerve fibers [7, 10]. Failure of either of the delicate processes of neurulation and disjunction can result in anchoring of the spinal cord to the surrounding tissues, thereby preventing the independent growth of the spinal cord. If the spinal cord cannot detach itself from the surrounding meninges, vertebrae, or subcutaneous tissues, the spinal cord cannot ascend relative to the vertebral column.

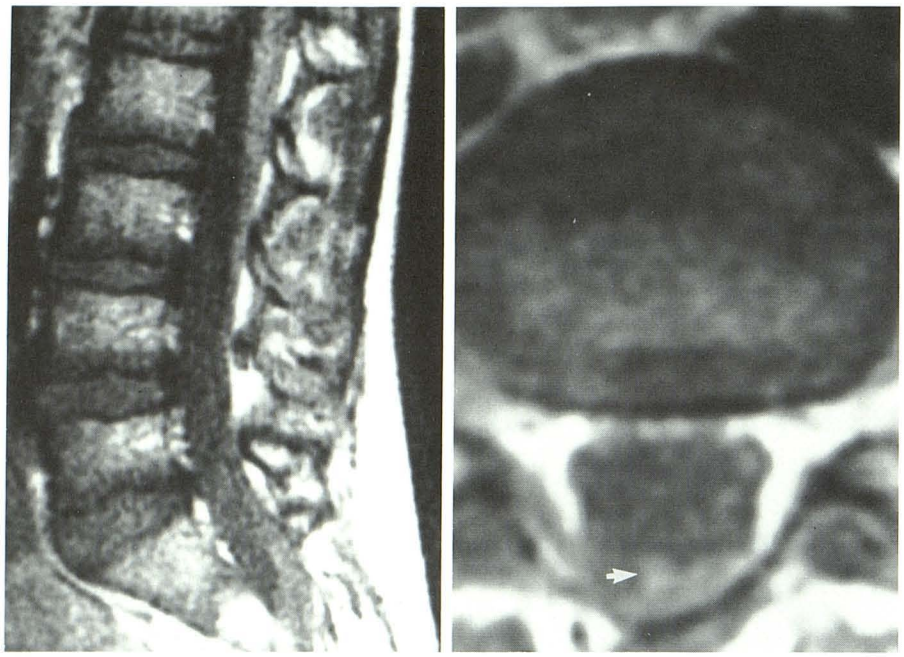

Fig. 4.—Case 20: 7-year-old girl with tethered spinal cord syndrome. Tip of conus is at lower L3 vertebral level.

***A*, Sagittal spin-echo image, 1000/20, does not show filum terminale clearly.**

***B*, Axial spin-echo image, 1000/20, at L5–S1 interspace. Filum terminale (*arrow*) is 4 mm thick.**

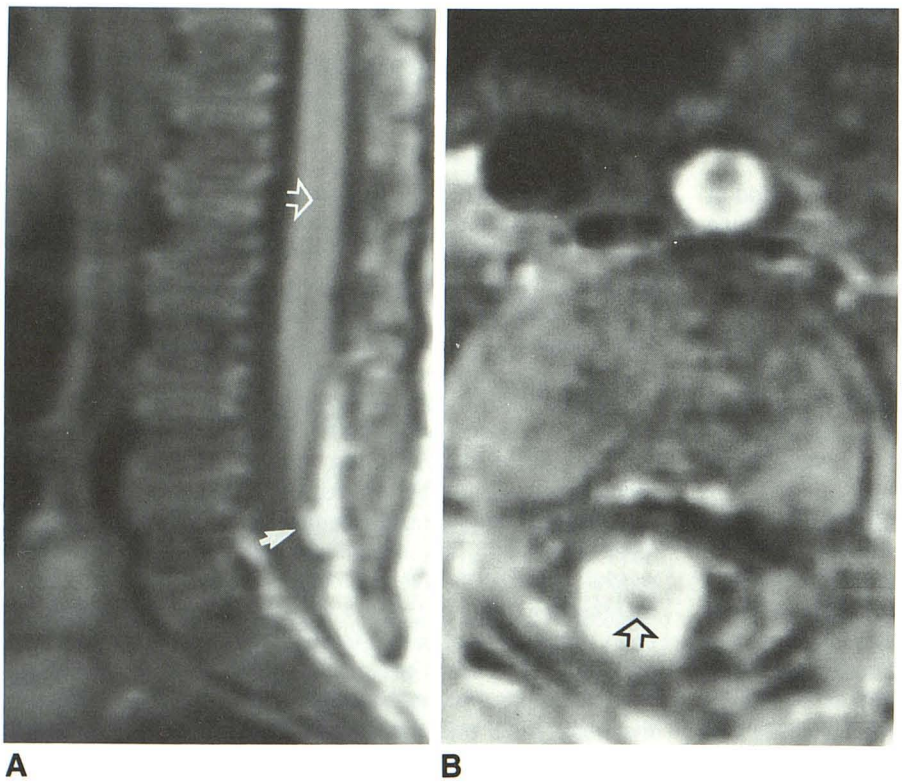

Fig. 5.—Case 9: 3-week-old boy with fatty mass over lumbosacral spine and neurogenic bladder.

***A*, Sagittal spin-echo image, 1000/20, reveals termination of cord in lipoma (*solid arrow*) at L3–L4 level. Linear low intensity (*open arrow*) within cord contour was believed to be artifactual.**

***B*, Axial spin-echo image, 600/20, through L2 vertebral body clearly identifies central syringohydromyelic cavity/myelomalacia (*arrow*). Lesion was very focal and was not as extensive on axial scans as would have been suggested by linear intensity on sagittal image.**

More rapid growth of the spinal column relative to the cord then results in tethering [11, 14].

Disturbance in the closure of the neural placode during neurulation with nondisjunction results in myelomeningocele [12]. The edges of the exposed placode blend with a thin membrane that connects to the surrounding margins [7]. Dorsal dermal sinuses appear to arise from focal incomplete separation of cutaneous ectoderm from neuroectoderm [7]. Focal premature disjunction with exposure of paraxial mesoderm to the dorsal aspect of unfused neural ectoderm induces

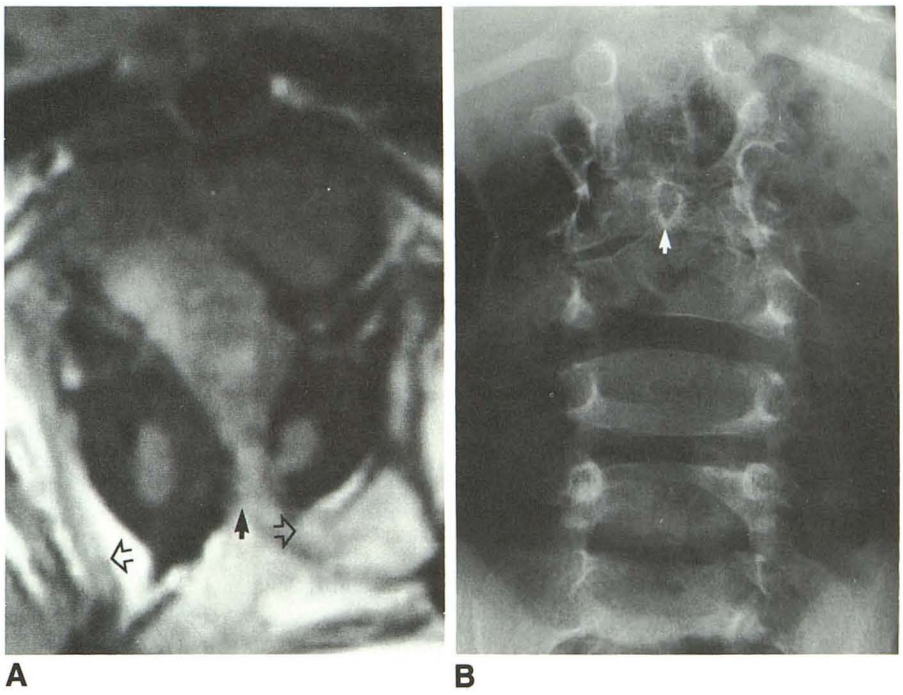

Fig. 6.—Case 24: 5-year-old boy with tethered spinal cord syndrome.

***A*, Axial spin-echo image, 1000/20, through lower thoracic spine clearly reveals diastematomyelia with septum (*solid arrow*). Thickened everted laminae (*open arrows*) are evident.**

***B*, Conventional radiograph of lower thoracic upper lumbar spine confirms bony nature of diastematomyelic septum (*arrow*).**

formation of fatty elements, which may prevent fusion of the neural tube and result in the formation of cord lipomas and lipomyelomeningoceles [13]. The fatty mass may attach to the meninges, vertebrae, muscle, or skin. Diastematomyelia is thought to develop from the persistence of an accessory neurenteric canal, which prevents midline fusion of the neural tube [15], or alternatively from formation of two neural tubes as a result of the neural folds turning back ventrally instead of fusing as they approach midline [7]. The presence of a fibrous or bony septum between the hemicords, fibrolipomas at the dorsal aspect of the cleft, adhesions between the hemicords and the meninges, or thickened filum terminale may result in tethering in diastematomyelia [7].

The tight filum terminale syndrome is by definition tethered spinal cord syndrome associated with a short, thickened filum terminale and a low-lying conus. Theoretically the lack of filum elongation from faulty retrogressive differentiation may result in a longer spinal cord, but this in and of itself should not result in cord tethering. Sarwar et al. [16] have postulated that a hemorrhagic or inflammatory insult to the caudal cord may result in reparative elastic or fibrofatty bands that may retract on healing, resulting in tethering of the spinal cord.

The spinal cord is a viscoelastic structure that is fixed and buffered by the dentate ligaments and the filum terminale [17]. The compliance of the filum terminale is far greater than any spinal cord segment and protects the cord from stretching [18]. When the filum is thickened, this protective effect is lost. Elongation of the cord is greatest near the point of tethering [17].

Yamada et al. [19] demonstrated that stretching of the cord results in a highly reduced state of mitochondria, thereby decreasing production of adenosine triphosphonate. Tethering results in stretching, distortion, or kinking of arterioles, venules, and capillaries, but it is unclear if metabolic defects are secondary to ischemia or to some other factor relating to physical stretching of the spinal cord [11]. In any case, metabolic impairment results in functional deterioration of nerve cells. The perikarya (nerve cell bodies) are affected earlier than axons are, and this may account for the earlier appearance of incontinence, muscle atrophy, and hyporeflexia, as opposed to long tract signs such as hyperreflexia and the Babinski sign. Cell damage is reparable up to a point; therefore untethering may result in clinical improvement if the mitochondria are not damaged irreversibly [11].

Repeated acute stretching of the spinal cord may also accentuate the oxidative metabolic changes caused by chronic tethering. The tethered spinal cord syndrome usually presents in childhood, but may present in adults when precipitated by an acute event such as additional tugging when in the lithotomy position, narrowing of the spinal canal by a disk, or direct trauma to the back or buttocks [20]. Twenty-nine percent of our patients were older than 35 years of age.

MR permitted us to confirm the presence of and define the cause of the tethered spinal cord in each case. Myelomeningoceles are obvious clinically and usually are repaired shortly after birth. The majority of patients with skin-covered spinal dysraphisms such as lipomyelomeningoceles are neurologically normal at birth [4, 11]. This may account for the fact that in our series patients undergoing preoperative MR imaging tended to be older and predominantly had skin-covered spinal dysraphisms. Spinal lipomas were the most common traction lesions.

Identification of the level of the conus was concordant in 17 of 19 patients on both sagittal and axial images. In the

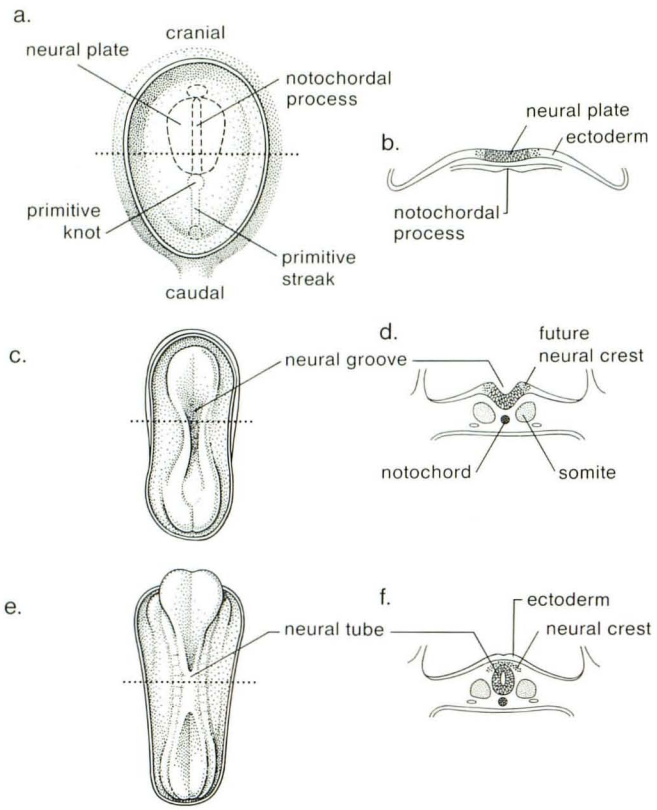

Fig. 7.—Neurulation and disjunction. Dorsal (*a*, *c*, and *e*) and transverse (*b*, *d*, and *f*) sections.

***a* and *b*, Thickening of embryonic ectoderm is seen dorsal to notochord to form neural plate.**

***c* and *d*, Neural plate invaginates along its central axis to form neural groove.**

***e* and *f*, Neural folds fuse dorsally to form neural tube (neurulation) and simultaneously separate from surface ectoderm (disjunction). First fusion of neural folds is at level of third or fourth somite, and then fusion progresses both cranially and caudally.**

(Modified from [8, 9], with permission.)

other two cases, the location on sagittal views was discrepant by at least one vertebral body height from that on axial views. In one case, differentiation of conus from cauda equina was superior on the axial images; the tip of the conus was interpreted as being more cephalad than was suggested on the sagittal study. The inferiorly pointed appearance of the conus usually is readily distinguishable from cauda equina on median sagittal images. However, on sagittal sections slightly off midline, the tip of the conus may be difficult to separate from the roots of cauda equina, which may appear as a uniform structure. Axial images may then be used to confirm the location of the conus termination (Fig. 8) [21]. In the remaining case, the caudal portion of the cord was displaced laterally by a lipoma. Therefore, it was difficult to identify the level of termination of the conus on the sagittal views; the axial images revealed the conus tip to be lower by one vertebral body height (Fig. 1). In all instances, the conus level was assessed more easily and better differentiated from the surrounding cauda equina on axial than on sagittal images.

In 16% of our cases, the tip of the conus was in a normal position. The radiographic diagnosis of tethered spinal cord in these patients had to be determined on the basis of abnormal filum or the presence of a tethering lesion. The thickness of the filum was very useful in the assessment of these patients. We found an abnormally thick filum (greater than 2 mm) at the L5–S1 level in 15 of the 16 patients in whom this measurement could be made. In the patient with a filum thickness of 2 mm, the conus was low-lying. Therefore, the diagnosis of tethered cord was possible even when the filum thickness was normal. Measurements were performed at the L5–S1 interspace level rather than at more cephalad levels, where the filum may appear normal in size due to stretching [11].

A fatty filum terminale was noted as an incidental finding in an additional two patients (33 and 38 years old) whose symptoms could be explained by disk herniations (Fig. 9).

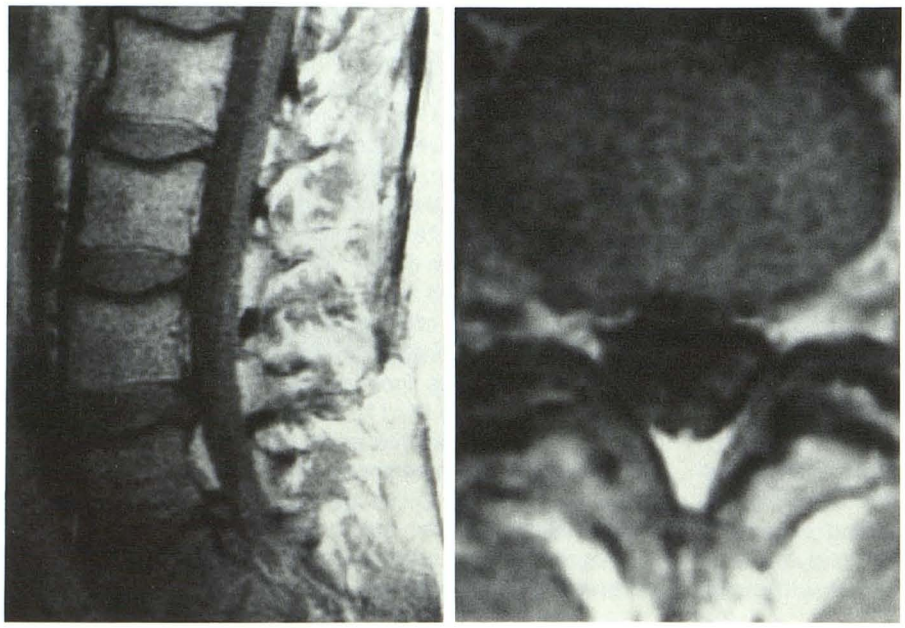

Fig. 8.—Case 12.

***A*, Slightly off-center sagittal spin-echo image, 1000/20. Cauda equina nerve roots are so uniform as to be confused with conus.**

***B*, Axial spin-echo image 1000/20, confirms presence of cauda equina roots rather than tip of conus at L3–L4 level. Tip of conus was opposite mid L1 vertebral body.**

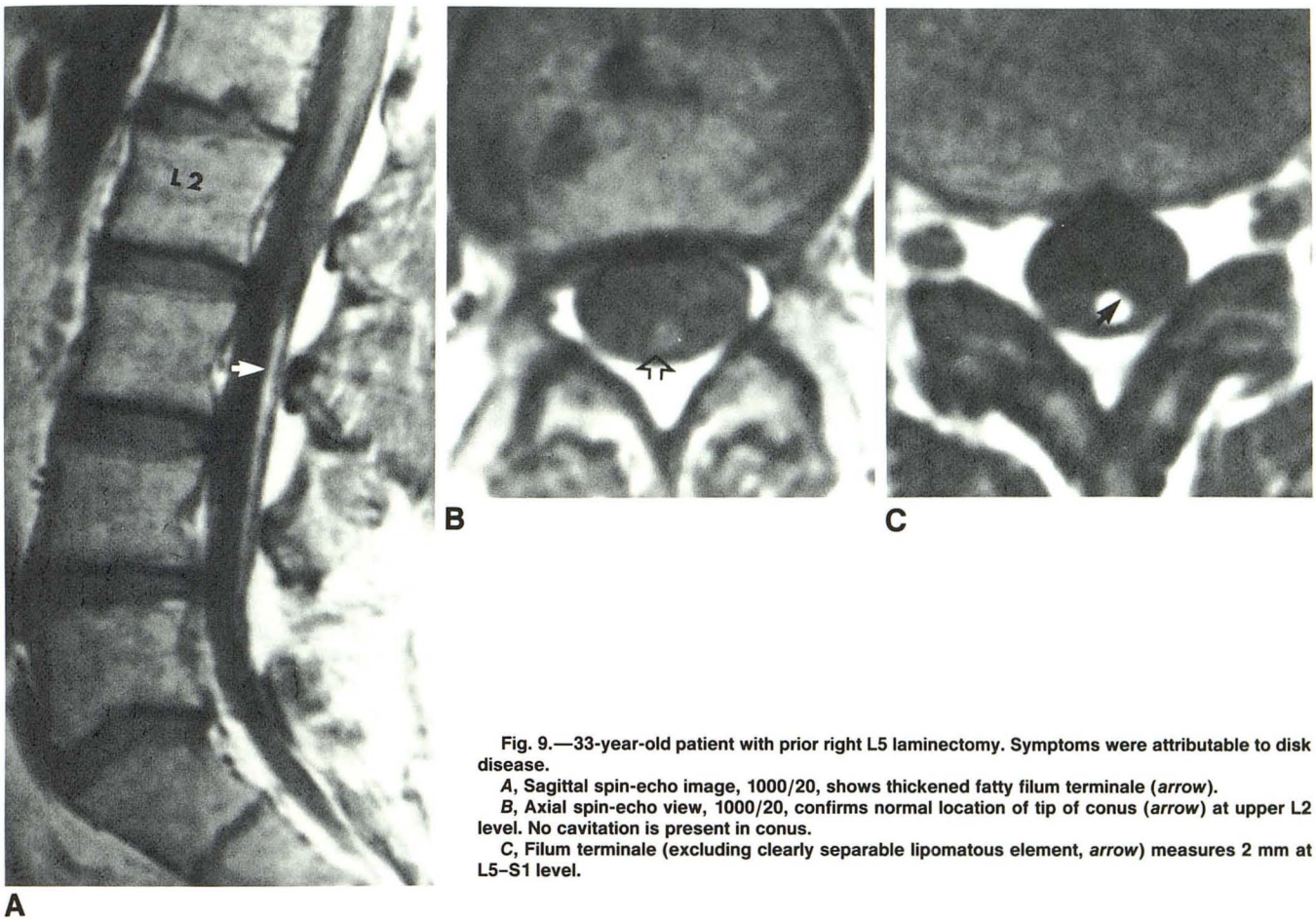

Fig. 9.—33-year-old patient with prior right L5 laminectomy. Symptoms were attributable to disk disease.

***A*, Sagittal spin-echo image, 1000/20, shows thickened fatty filum terminale (*arrow*).**

***B*, Axial spin-echo view, 1000/20, confirms normal location of tip of conus (*arrow*) at upper L2 level. No cavitation is present in conus.**

***C*, Filum terminale (excluding clearly separable lipomatous element, *arrow*) measures 2 mm at L5–S1 level.**

Although tethering may remain subclinical until aggravated by factors that further increase the tension [20], none of the other radiographic criteria of tethered cord were satisfied in either patient. The filum terminale was 2 mm or less in thickness at the L5–S1 level, the conus was above the mid L2 level, and no syringohydromyelic cavity/myelomalacia was identified in the lower spinal cord. Therefore, fatty filum terminale, a possible result of faulty retrogressive differentiation, may not in and of itself be an important radiographic indicator of a tethered spinal cord.

In this study, we did not compare the efficacy of CT with intrathecal contrast material and MR. The inherent advantages of MR are that it is noninvasive and there is no ionizing radiation. Anatomic definition and characterization of the tethering lesions (i.e., lipoma), neural placode, and nerve roots are, in our experience, superior with MR. Flow-compensation gradients and small flip-angle techniques should further improve image quality and nerve root detail by reducing imaging times (less motion artifact) and producing artifact-free myelographic effects. Poor bone definition has always been described as a major limitation of MR compared with CT. In 19 of the 25 patients in our series, the bony dysraphic changes were demonstrated easily. We were able to identify a bony spur and other associated bony changes such as thickened, everted laminae and hemivertebrae in a patient with diastematomyelia (Fig. 6). Vertebral osseous abnormalities are more readily identified and characterized on CT. Identification of neural elements, however, is the primary goal in the evaluation of these patients.

Previous reports have not commented on the association of syringohydromyelia/myelomalacia and tethered spinal cord syndrome except as a postoperative complication or as an additional finding with Chiari malformation [11]. Nine patients in our series had a small, low-intensity cord lesion near to and extending from the conus or the tethering lesions. The syringohydromyelia/myelomalacia could be diagnosed with confidence only on axial images; interpretation on sagittal views was hindered by truncation (Gibbs) and partial-volume artifacts. Given that no axial images were available in five patients, syringohydromyelia/myelomalacia was actually noted in nine of the 20 patients who were adequately evaluated. Six of the nine patients were 11 years old or younger. These small cord lesions probably could not have been detected by any other imaging method. The numbers in this study are small and further experience is necessary, but it is possible that such mild syringohydromyelia/myelomalacia may be a useful ancillary sign in the radiologic diagnosis of tethering.

Stretching of the spinal cord is most prominent in the segment adjacent to the traction lesion [17]. With tethering, oxidative metabolism of the cord is impaired, arterioles and

venules are stretched and distorted, and electron microscopy reveals wrinkling and tearing of the cell membrane [11]. A combination of these factors may be the basis of intramedullary cavity formation. According to the above-proposed mechanism, the cord probably has to go through a stage of myelomalacia (cord softening) before proceeding to actual cavitation [22]. Because we do not have pathologic proof and because a small focus of myelomalacia can be difficult to differentiate with confidence from a small syringohydromyelic cavity on MR, we have referred to the low-intensity cord lesion as syringohydromyelia/myelomalacia.

It is unclear what contribution the focal syringohydromyelic cavity/myelomalacia makes to the symptom complex of tethered spinal cord syndrome and how it may affect the prognosis of treatment. After surgery for tethered cord, motor improvements are seen in 50% of patients, with improvement of urologic function in only 7%. Many deficits stabilize but do not improve [11]. Early prophylactic care is therefore the standard, even in asymptomatic children [4]. The presence of the low-intensity cord lesion may denote some form of irreversibility. Postsurgical follow-up was available in six patients. One of the two patients who remained asymptomatic had a low-intensity focus in the conus. In two patients, symptoms stabilized, and syringohydromyelia/myelomalacia was noted in the one with persistent neurogenic bladder; the other had a hemispastic gait. Syringohydromyelia/myelomalacia was identified in the spinal cords of both of the remaining two patients: one eventually became hemiplegic and the other developed progressive calcaneovalgus deformity.

From a diagnostic point of view, the presence of syringohydromyelia/myelomalacia can be a helpful adjunct when the conus is not low-lying and the diagnosis of tethered spinal cord is clinically suspected. One of our six patients with tethered spinal cord syndrome and a normal conus level had a minimally thickened filum terminale (3 mm) and a low-intensity lesion in the conus.

In summary, MR is very useful in visualizing the conus medullaris, assessing the thickness of the filum terminale, and identifying traction lesions in a patient clinically suspected of having tethered spinal cord syndrome. Associated bony dysraphisms are easily evaluated. We noted a frequent occurrence of focal syringohydromyelia/myelomalacia near the tip of the conus or in the cord near the tethering lesion. This may be a useful diagnostic sign but the prognostic significance is unclear.

REFERENCES

1. Barson AJ. The vertebral level of termination of the spinal cord during normal and abnormal development. *J Anat* **1970**;106:489–497
2. Smoker WRK, Godersky JC, Knutzon RK, Keyes WD, Norman D, Bergman W. The role of MR imaging in evaluating metastatic spinal disease. *AJR* **1987**;149:1241–1248
3. Masaryk TJ, Modic MR, Geisinger MA, et al. Cervical myelopathy: comparison of magnetic resonance and myelography. *J Comput Assist Tomogr* **1986**;10:184–194
4. Edwards MSB. Management of lipomyelomeningoceles in childhood. *Int Pediatr* **1987**;2:120–123
5. James CCM, Lassman LP. *Spinal dysraphism: spina bifida occulta.* New York: Appleton-Century-Croft, **1972**:82–96
6. Fitz CR, Harwood-Nash DC. The tethered conus. *AJR* **1970**;125(3): 515–523
7. Newton TH, Potts DG, eds. *Computed tomography of the spine and spinal cord. Spinal dysraphism*, Vol. 1. San Anselmo, CA: Clavadel, **1983**: 299–354
8. Moore KL. *The developing human*, 4th ed. Philadelphia: Saunders, **1988**:48–51
9. Cowan M. The development of the brain. *Sci Am* **1979**;241(3):112–133
10. Lemire RJ, Loeser JD, Leech RW, Alvord EC. *Normal and abnormal development of the human nervous system.* New York: Harper & Row, **1975**:54–83
11. Holtzman RN, Stein BM, eds. *The tethered spinal cord.* New York: Thieme-Stratton, **1985**:1–147
12. Osaka K, Matsumoto S, Tanimura T. Myeloschisis in early human embryos. *Childs Brain* **1978**;4:347–359
13. McLone DG. The subarachnoid space: a review. *Childs Brain* **1980**;6:113–130
14. Jones PH, Love JG. Tight filum terminale. *Arch Surg* **1956**;73:556–566
15. Bremer JL. Dorsal intestinal fistula; accessory neuroenteric canal; diastematomyelia. *Arch Pathol Lab Med* **1952**;54:132–138
16. Sarwar M, Virapongse C, Bhimani S. Primary tethered cord syndrome: a new hypothesis of its origin. *AJNR* **1984**;5:235–242
17. Sarwar M, Crelin ES, Kier EL, Virapongse C. Experimental cord stretchability and the tethered cord syndrome. *AJNR* **1983**;4:641–643
18. Tani S, Yamada S, Knighton R. Extensibility of the lumbar and sacral cord. *J Neurosurg* **1987**;66:116–123
19. Yamada S, Zinke DE, Sanders D. Pathophysiology of "tethered cord syndrome." *J Neurosurg* **1981**;54:494–503
20. Pang D, Wilberger JE. Tethered cord syndrome in adults. *J Neurosurg* **1982**;57:35–47
21. Monajati A, Wayne WS, Rauschning W, Ekholm SE. MR of the cauda equina. *AJNR* **1987**;8:893–900
22. Gebarski SS, Maynard FWS, Gabrielson TO, Knake JE, Latack JT, Hoff JT. Post-traumatic progressive myelopathy. *Radiology* **1985**;57:379–385